Control of end-of-life oxygen-containing groups accumulation in biopolyesters through introduction of crosslinked polysaccharide particles

SCHOLARONE™
Manuscripts

Control of end-of-life oxygen-containing groups accumulation in biopolyesters through introduction of crosslinked polysaccharide particles

Clelia Dispenza, Maria Antonietta Sabatino, Giulia Infurna, Nadka Tz. Dintcheva*

Dipartimento di Ingegneria, Università di Palermo, Viale delle Scienze, Ed. 6, 90128 Palermo, Italy

Abstract

The gradual release of fossil-based sources to produce polymers and the development of bio-based materials is a trend undertaken by several current research programmes and initiatives for sustainable development. Therefore, the formulation of bio-based materials, having good properties and performance in service and controlled end-of-life, is imperative for an effective circular economy. In this work, an innovative approach to induce and control the end-of-life of biodegradable polyesters through introduction of crosslinked polysaccharide particles, that do not change main biopolyester properties, is proposed. Chitosan has been subjected to ionotropically crosslinking to obtain micro-/nano-particles, and then, the particles have been introduced into PolyLactic Acid (PLA) by melt mixing. The obtained results suggest that the introduction of crosslinked chitosan particles do not change the PLA glass transition, cold crystallisation and fusion phenomena, while the introduction of untreated chitosan modifies significantly the PLA thermal behaviour. Infrared and UV-visible spectroscopic data highlight that no changes occur for PLA due to addition of both untreated and crosslinked chitosan. Finally, thin PLA-based films have been subjected to artificial accelerated UVB exposure to monitor the accumulation of oxygen-containing groups. Interestingly, at low exposure time, the presence of chitosan slows down the accumulation, while at long exposure time, it induces accelerated oxygen formation, supporting its beneficial effect as end-of-life accelerant.

Keywords: ionotropically crosslinked chitosan; oxygen-containing groups accumulation; PLA photodegradation

---

* Corresponding author. Tel: +39 091 23863704. E-mail address: nadka.dintcheva@unipa.it (N.Tz. Dintcheva).

1. Introduction

The formulation of bio-based materials from naturally occurring sources is a very challenging issue related to the gradual release of fossil-based sources, the development of bio-based industry and the implementation of circular economy [1,2]. Although replacing of fossil-based polymers by biopolymers may have positive impacts on the environment and human health, the production of biopolymers at large industrial scale is still a challenge. Certainly, in the next decade, the attention of researchers will be more and more focused on formulation and production, especially at large industrial scale, of bio-based materials having suitable properties and performance, similar to those of synthetic polymers [1,3–5].

Polylactic acid (PLA), as well known, is one of the most attractive biodegradable polymers because of the natural origin of monomers, its compostability and biodegradability, and other properties that make it a good candidate in replacing fossil-based polyolefins for some industrial applications [1,2,6–9]. As also widely documented, neat PLA shows inferior thermal and thermo-mechanical resistance compared to many petroleum-based polymers. Therefore, to improve its thermal and mechanical performance, it is often mixed with various additives, such as natural clay, metal oxides, natural fibres, etc. The presence of these additives can increase thermal stability, hardness and rigidity, reducing its ductility [10–13]. Unfortunately, biodegradation can be penalised by the presence of many of those additives, when they slow down the formation and accumulation of oxygen-containing groups in the polymer [10,14].

According to the literature, the PLA biodegradation process requires specific environmental conditions, *i.e.* temperature ca. 70°C, relatively high humidity, time up to 90 days for samples having thickness lower than 200 microns, and the presence of microorganisms [15]. It proceeds mainly by chain scission and accumulation of oxygen-containing groups on the chain fragments that facilitate the polymers deterioration by microorganisms [7,16,17]

In the past, to control oxygen-containing groups accumulation and subsequent end-of-life degradation of the polyolefins, the addition of appropriate pro-oxidant substances, such as metal-based complexes, was proposed. Unfortunately, this approach cannot be considered a viable solution at a large scale due to the potential negative environmental impact of most of these substances [18–20]. The degradation process of polymers and biopolymers can be accelerated by adding large amounts of natural clay, containing metal impurities [21–23] or pro-oxidant additives [20].

For the opposite goal, that is to improve the oxidation resistance of biopolymers, several natural antioxidants, such as phenols, polyphenols, carotenoids, vitamins, etc., can be added during manufacturing. Interestingly, some of them exert concentration-dependent anti-/pro-oxidant activity. Indeed, if natural antioxidants are added at high concentration to a biopolymer matrix, they can actually exacerbate the oxidation phenomena, rather than having protection action. This issue has

been documented for some carotenes in the past, and currently also for some phenols and polyphenols [18,19,24].

Chitosan is a cationic polysaccharide obtained by controlled deacetylation of chitin, a polysaccharide present in the exoskeleton of crustaceans, fungal cell walls and other biological materials [25]. Chitosan properties and performances depend on the deacetylation degree and molecular mass [26,27]. If added as polymeric filler of PLA, chitosan can effectively improve the mechanical and barrier property of the composite films [28–30]. Due to its intrinsic biocompatibility, biodegradability and non-toxicity [31–33] chitosan has been extensively studied for applications in drug delivery [34], as edible coating for food [25,35] and transparent films for cultural heritage protection [36], where the high permselectivity to CO_2 and O_2 is also very beneficial [25,37].

In this work, an innovative approach to induce and control end-of-life oxygen-containing groups accumulation in a biopolyester, such as PLA, without modification of its main properties, is proposed. Specifically, ionotropically crosslinked chitosan micro-/nano-particles were synthetised and introduced into the PLA matrix at different concentrations thorough melt mixing, and their effect on PLA thermal behaviour, spectroscopic properties and oxygen-containing groups accumulation has been evaluated. The PLA-based films containing ionotropically crosslinked chitosan micro-/nano-particles at different concentrations were subjected to artificial UVB exposure and the oxygen-containing groups accumulation was monitored in time through infrared spectroscopical analysis.

2. Experimental part

2.1. Materials

The materials used in this work are:

- PolyLactic Acid (PLA) 3001D has been purchased by NatureWorks LLC. Its main properties are: injection molding sample with melting point = 200 °C; heat distortion temperature = 55 °C; melt flow rate (210 °C / 2.16 kg) = 22; clarity – transparent.

- Low molecular weight chitosan with deacetylation degree in the range 75-85% has been purchased by Sigma Aldrich.

- Glacial acetic acid, hydrogen chloride 37% (HCl) and disodium sulphate has been purchased by Sigma Aldrich.

2.2. Preparation of ionotropically crosslinked chitosan micro/nano-particles

In consideration of the large molecular weight distribution of the chitosan, the low molecular weight fraction was removed by dialysis. In particular, a 1% w/v aqueous solution of the polymer in 0.20 % w/v acetic acid and 0.01M HCl was prepared at room temperature by magnetic stirring for 24 h. The solution was then dialyzed against its own solvent (0.20 % w/v acetic acid and 0.01M HCl) for three days using a 12kDa cut-off dialysis membrane. The solution was then freeze-dried. After this treatment, a fraction corresponding to the $33.0 \pm 4.0\%$ of the total polymer was removed. The dry polymer was then redispersed in bi-distilled water containing 2.0 %w acetic acid at 0.1 w/v, by magnetic stirring for 2 h. To a given volume of each solution a proper amount of 10% w/v disodium sulphate solution was added in order to keep the polymer to salt weight ratio always equal to 0.1. The addition was performed dropwise in an ultrasound bath at 25°C. After addition of the salt, the final mixture was sonicated for 10 minutes. The crosslinked chitosan particles were recovered by centrifugation at 13000 rpm per 30 minutes at 15°C to remove the surnatant solution containing the excess of salt, redispersed in water and filtrated with 5 μm cut-off syringe filters to remove eventual larger aggregates and, finally, dried in a vacuum oven at 40°C until constant weight was attained. No appreciable dry polymer weight change was measured.

2.3. Processing by melt extrusion

PLA pellets were dried before processing for 24 h under vacuum in an oven at 70 °C. The preparation of PLA-based samples was carried out using a a Haake Minilab Rheomex micro-compounder model CTW5 conical twin-screw extruder operating in a co-rotating mode. The processing temperature was 170°C, the residence time 5 minutes and the rotation speed was 100 rpm. Both untreated chitosan and crosslinked chitosan particles were added at 1.0 %w and 1.0, 2.0 and 4.0 %w, respectively, to the polymer melt after 2 minutes of processing. Neat PLA was subjected to the same processing condition.

Thin films (thickness about 60 μm) of neat PLA and PLA-based systems containing chitosan were obtained through compression molding (for 5 minutes at 6000 psi) in a Carver Laboratory Press.

2.4. Characterizations

2.4.1. Differential Scanning Calorimetry (DSC)

The calorimetric data were evaluated by differential scanning calorimetry (DSC) using a Perkin-Elmer DSC7 calorimeter. All experiment were performed under dry N_2 on samples of around 10 mg in 40 μl sealed aluminium pans. Four calorimetric (two heating: 30-200 °C and two cooling: 200-30 °C) scans were performed for each sample at scanning heating/cooling rate of 10 °C/min.

2.4.2. Thermal-gravimetric analysis (TGA)

Thermal-gravimetric analysis (TGA) was conducted with STA6000 Perkin–Elmer apparatus. Samples were tested in a temperature range of 30−600 °C at a heating rate of 10 °C/min under nitrogen flux (20 ml/min). The characteristic temperatures associated to the various phenomena are calculated as the peak temperature of the first derivative function (DTG).

2.4.3. Scanning Electron Microscopy (SEM)

SEM analysis was performed on cryogenically fractured and gold sputtered surfaces of thin films using a Philips (Netherlands) ESEM XL30 scanning electron microscope.

2.4.4. Fourier Transform Infrared Analysis (FTIR)

A Fourier Transform Infrared Spectrometer (Spectrum One, Perkin Elmer) was used to record IR spectra using 16 scans at a resolution of 1 cm^{-1}. Measurements were obtained from the average of triplicate samples with a calculated maximum experimental error (relative standard deviation) of around 5%.

The progress of degradation for PLA and PLA-based systems has been followed by running FTIR analysis with time and monitoring the variations in the range 1800-1700 cm^{-1} in time, using Spectrum One software.

2.4.5. UV-visible Analysis (UV-vis)

UV-visible Spectrometer, (Specord®250 Plus, Analytikjena), was used to record UV-Vis spectra performing 8 scans between 200 and 1100 nm at a resolution of 1 nm.

2.5. Photo-oxidation exposure

Photo-oxidation tests of PLA and PLA-based films (thickness about 60 μm) were carried out using a Q-UV/basic weatherometer (from Q-LAB, USA) equipped with UVB lamps (313 nm). The weathering conditions were a continuous light irradiation at T = 55 °C. The progress of photo-oxidative degradation was followed by FTIR spectroscopic technique.

3.   Results and discussion

3.1.   Ionotropically crosslinked chitosan micro/nano-particles

In order to evaluate the thermal resistance of the ionotropically crosslinked chitosan, the thermogravimetric analysis of chitosan (Ch) and crosslinked chitosan (cCh) was carried out. The obtained thermograms are plotted in Figure 1a, it is wort noting that both Ch and cCh samples were dried for 24h at temperature of about 80 °C in a vacuum oven before the analysis. In the thermogram of Ch, a first weight loss of ca. 5 % w is observed in the temperature range between 50°C and 100 °C, mainly due to evolution of bound water. Evidently, the dehydration treatment that was carried out before analysis removed only plasticising (unbound) water, *i.e.* only free water present between polymer chains, while did not remove adsorbed bound water, *i.e.* water that is physically or chemically interacting with polymer chains. The material is thermally stable up to ca. 250 °C when a relatively steep weight loss process takes place in the temperature interval between 250 and 300 °C, corresponding to an overall weight loss of ca. 40 %. This weight loss is caused by the main pyrolytic degradation of chitosan caused by the random split of the glycosidic bonds, accompanied by the release of low molecular weight compounds (H_2O, NH_3, CO, CO_2 and CH_3COOH) and significant structural rearrangements of the polymer chain segments (decomposition of pyranose rings through dehydration and deamination first and then ring-opening reactions) [38]. At ca. 450°C the thermogram curve slope changes, becoming much less steep and causing a relatively modest further weight loss (ca. 40 %) in the temperature interval between 450 °C and 600 °C. The overall residual weight is of about 36 % at 600 °C. According to the literature, this second step of the thermal degradation process is associated to CH_4 evolution and consequent formation of a graphite-like structure via dehydrogenation mechanism.

The thermogram of cCh clearly shows that the sample possesses a lower amount of bound water. This behaviour has been already observed for other ionically crosslinked polyelectrolytes characterised by a relatively high crosslinking density. In our system, it can be ascribed to both the reduction of the number of hydrophilic groups available to establish direct interactions with water molecules, some being engaged in ion-ion bonds with dissociated potassium sulphate ions, and to the restricted mobility of the ones that are not involved in crosslinks. On the other hand, crosslinking can increase the portion of amorphous regions of the polymer and create cavities inside the material, thus favouring the access of free, unbound water. This water was probably successfully removed by the thermal treatment under vacuum. Another noticeable difference with respect to the thermogram of Ch is that weight loss associated to thermal degradation is anticipated to 200°C but is much less significant. Indeed, the final residual weight at 600 °C is of about 77 %. The decomposition reactions starting at lower temperatures likely involve loose chain ends of the network, while the crosslinked portions undergo progressive carbonization without significant low fragmentation. It is worth

highlighting that according to literature the main decomposition processes for chitosan are radical reactions, that can also evolve toward radical-radical combination, hence crosslinking. It has to be noted that a small portion of the residual weight at 600 °C can be attributed to the presence of the salt. In conclusion, the ionotropic crosslinking of chitosan has the advantage of reducing the amount of bound water, in comparison to the untreated chitosan, and this could mitigate the hydrolytic degradation for the host PLA matrix during melt processing at hight temperature, i.e. up to ca. 200 °C.

Figure 1b shows the scanning electron micrograph of the freeze-dried powder of crosslinked chitosan. Nanoparticles with an elongated shape are visible, glued together probably by the fraction of the polymer that is not crosslinked that was evidenced also by the thermogravimetric analysis.
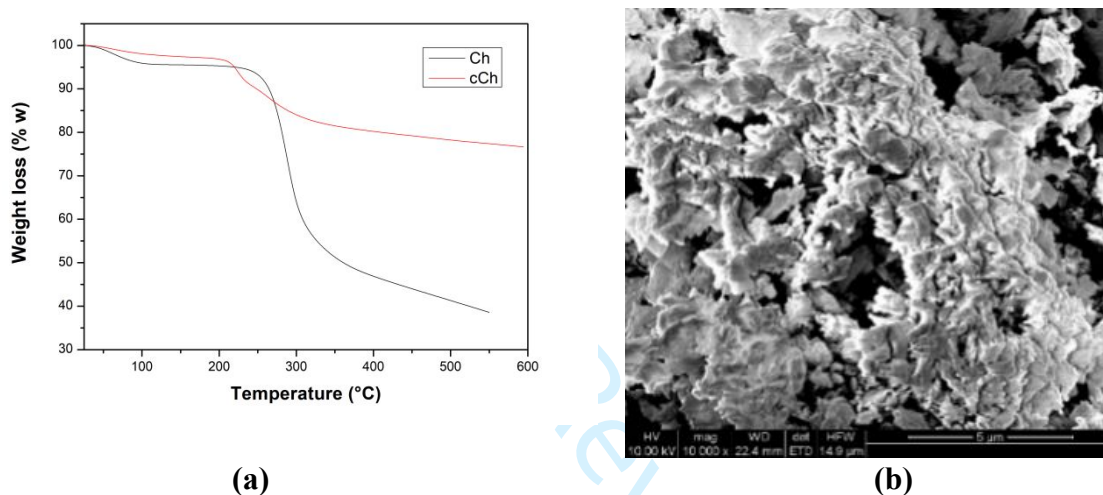

(a)   **(b)**

Figure 1. (a) TGA curves of untreated chitosan, Ch, and crosslinked chitosan, cCh, (b) SEM micrographs of crosslinked chitosan micro/nano-particle cluster

3.2.   *PLA / ionotropically crosslinked chitosan micro/nano-particles*

PLA-based samples containing 1.0 %w untreated chitosan and 1.0, 2.0 and 4.0 %w crosslinked chitosan were prepared by melt mixing, and then characterized by differential scanning calorimetry and thermogravimetric analyses. In Figure 2, the second heating scans of different PLA-based samples containing untreated and crosslinked chitosan micro/nano-particles at different concentrations are plotted. Besides, in Table 1, all information extracted from DSC curves (second heating scans), related to PLA glass transition (g), cold crystallization (cc) and fusion (f) are reported. We note that the introduction of 1 %w Ch leads to an anticipation of the glass transition phenomenon, *e.g.* the onset and offset temperatures are slightly lower than the corresponding values of neat PLA. Additionally, the presence of Ch causes the disappearance of cold crystallization phenomena and a significant reduction of the enthalpy of fusion of the crystalline domains to about 2.9 J/g against 43.7 J/g of neat PLA. The latter could be understood considering that the dispersed chitosan macromolecules into PLA cause a total loss of its crystalline structure. Contrarywise, the introduction

of crosslinked chitosan micro/nano-particles in different amounts, *i.e.* from 1 %w up to 4 %w, does not significantly influence the occurrence of thermal transition phenomena, see Table 1. Both onset and offset temperatures of the glass transition phenomenon remain almost unchanged. The values of cold crystallisation enthalpy are only 10 % higher than those of neat PLA. Interestingly, the values of fusion enthalpy increase by increasing the cCh concentration, probably because the crosslinked chitosan nano/microparticles dispersed in the matrix play a nucleation role in the formation of PLA crystalline structures. To sum up, the presence of chitosan blended with PLA has a negative effect on the thermal behaviour and, more specifically, on the cold crystallisation and melting behaviour of PLA that is no longer exhibited by the material, suggesting a totally amorphous state for PLA, hence a material with poorer barrier property and thermal resistance. On the contrary, the presence of ionotropically crosslinked chitosan micro-/nano- particles do not have any significant effect on PLA crystallinity, preserving its mechanical properties as well as the service temperature [39–41].
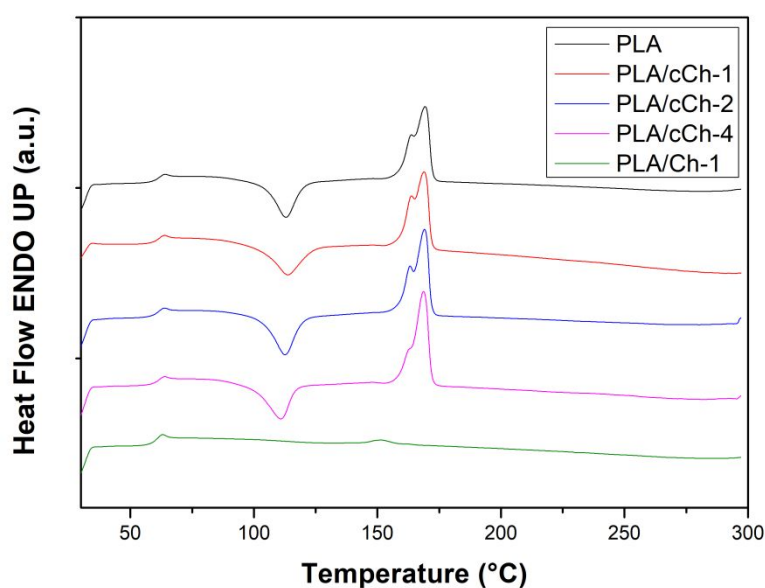

Figure 2. DSC curves, second heating scan, of neat PLA and PLA containing 1 %w untreated chitosan (Ch) and 1, 2 and 4 %w crosslinked chitosan micro/nano-particles (cCh)

Table 1. DSC data related to second heating scan, of neat PLA and PLA-based samples containing untreated chitosan (Ch) and crosslinked chitosan micro/nano-particles (cCh) at different concentration

Sample	Glass trans. (g)		Cold crystallisation peak (cc)				Melt peak (f)				
	Tg_{onset} [°C]	Tg_{offset} [°C]	Tcc_{onset} [°C]	Tcc_{offset} [°C]	Tcc_{peak} [°C]	ΔHcc [J/g]	Tf_{onset} [°C]	Tf_{offset} [°C]	Tf_{peak1} [°C]	Tf_{peak2} [°C]	ΔHf [J/g]
PLA	57.4	62.2	74.0	132.7	113.0	-38.9	148.0	181.8	163.7	169.3	43.7
PLA/Ch-1	57.0	60.9	-	-	-	-	134.6	172.4	151.5	163.4	2.9
PLA/cCh-1	57.6	62.1	71.5	133.4	113.7	-40.1	148.3	180.9	163.9	168.9	44.9
PLA/cCh-2	57.3	62.5	79.2	133.8	122.7	-42.6	148.1	178.4	163.2	169.0	47.4
PLA/cCh-4	57.9	62.9	77.6	132.7	110.8	-39.9	148.3	182.0	163.0	168.6	47.1

The TGA of selected PLA-based systems, namely PLA/cCh1 and PLA/cCh4, was carried out and the obtained thermograms are plotted in Figure 3. The thermogram of neat PLA is also reported for comparison. A single decomposition process can be seen for all systems. The onset decomposition temperature (T_d) is the same for neat PLA and PLA/cCh1 and the mass los at 600 °C is evaluated as 99.5 % for both PLA and PLA/cCh1. The PLA/cCh4 system appear slightly less thermally stable (lower T_d) and present a higher residual mass (ca. 2 %).
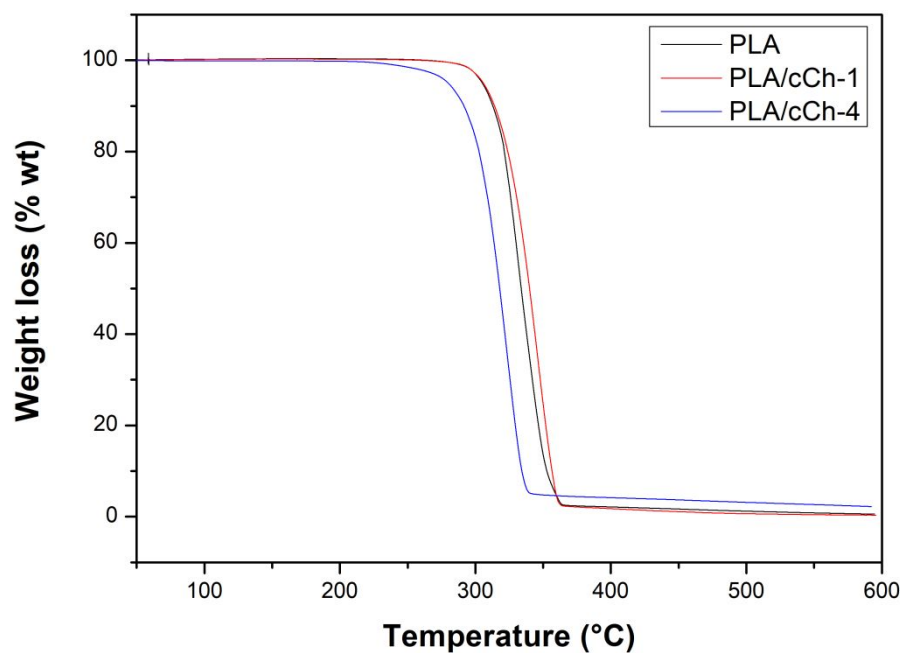

Figure 3. TGA curves of neat PLA and PLA containing crosslinked chitosan at different concentration

The fracture surface morphology of PLA/cCh composites was investigated by SEM, alongside with the fracture surfaces of PLA/Ch and neat PLA samples for comparison. In Figure 4, representative micrographs are reported. The neat PLA sample shows smooth, laminated fractured surfaces, see Figure 4a, that confirm the known inherently stiff and brittle character of PLA.
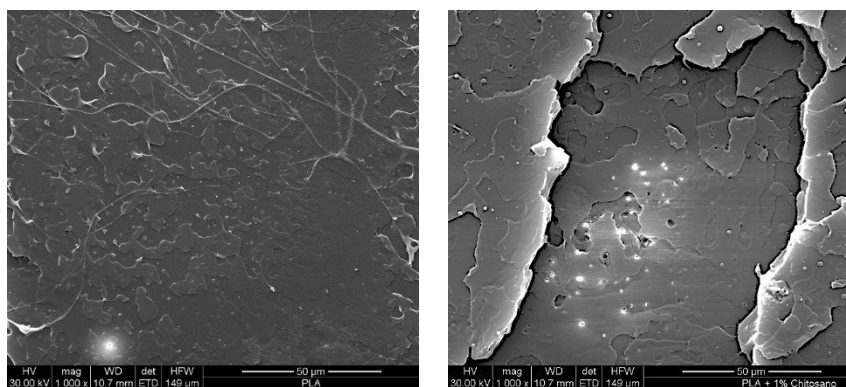
(a) PLA   *(b)PLA/Ch-1*
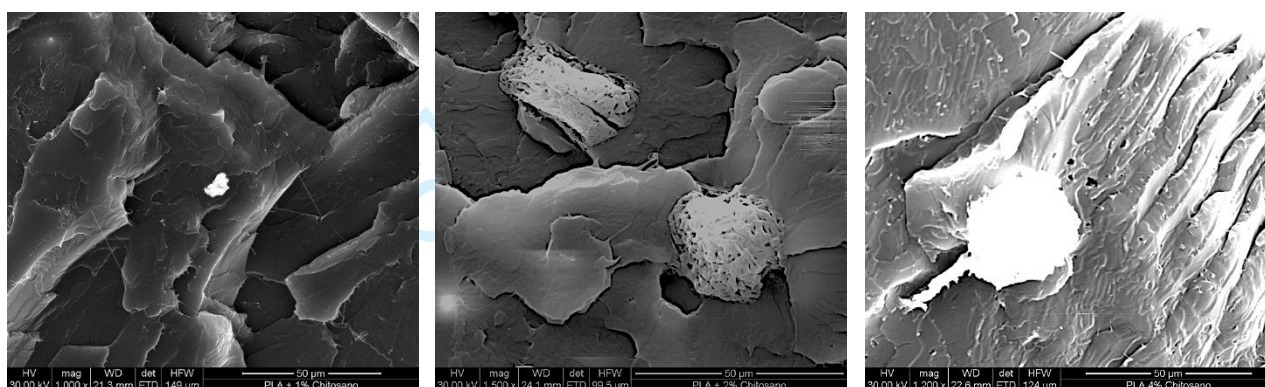
(c) PLA/cCh-1   *(d) PLA/cCh-2*   *(d) PLA/cCh-4*

Figure 4. SEM micrographs of different PLA-based samples

In Figure 4b, the micrographs of PLA blend with 1 %w untreated chitosan are shown. The fractured surface morphology appears less smooth than that of neat PLA. Several cracks and ridges are evident, which suggest that the presence of chitosan and its impact of PLA crystallinity has induced some ductile characteristics. In the micrographs of the PLA/cCh samples containing different cCh concentrations, i.e. 1 to 4 %w, we continue to observe a rougher fractured surface and the occasional presence of the larger particles (10-30 μm diameter), especially in the systems produced at higher cCh concentration, that are likely clusters of cCh nanoparticles. It is also worth noting that it appears to be good adhesion between the cCh micro/nano-particles clusters and the host matrix, see Figure 4c-e, suggesting compatibility between this biopolyester and the ionotropically crosslinked polysaccharide.

The chemical structure of PLA-based samples containing Ch and cCh was also investigated by FTIR and UV-visible spectroscopy analyses. In Figure 5, FTIR spectra, and according to literature, in Table 2, peaks assignment for pristine PLA [6] and pristine Ch [42] are reported. It is worth noting that no significant differences can be appreciated among the FTIR spectra of the various systems. Additionally, the main absorption bands of PLA and of Ch are overlapped, and for this reason, the presence of Ch and cCh in PLA cannot be detected by FTIR technique.
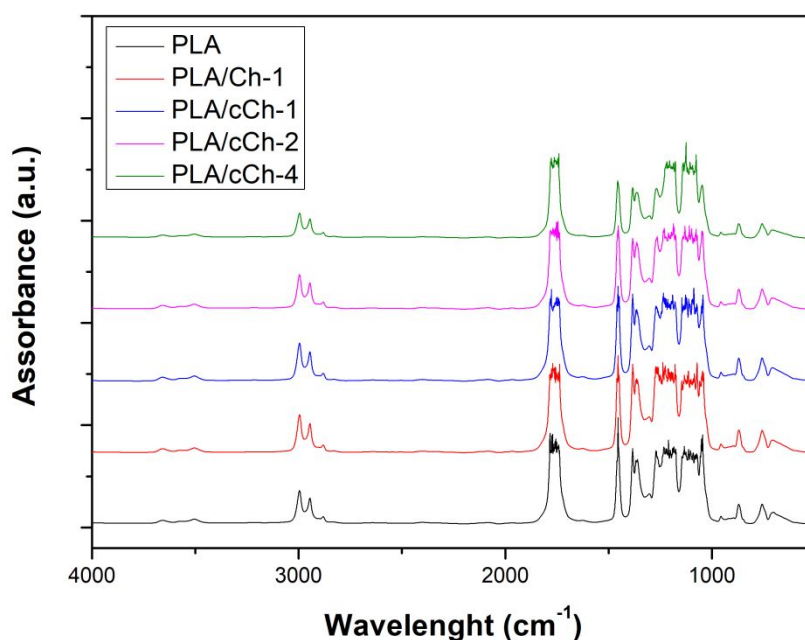
Figure 5. FTIR spectra of pristine PLA and PLA-based samples containing Ch and cCh

Table 2. Assignment of FTIR peaks for neat PLA [6] and neat Chitosan [42]

	PLA		Chitosan
v cm^{-1}	*Attribution*	v cm^{-1}	*Attribution*
3500	-OH stretching (free)	2927	symetric C-H stretching
2993,2879	-CH asym & sym stretching	1736	>C=O stretching
1748	-C=O carbonyl stretching	1626	C=O of ion COO stretching of secondary amide group (amide I)
1450	-CH$_3$ bending	1530	N-H bending (residue of amide II)
1382,1357	-CH- sym & asym bending	1395	C=N stretching (amide III band)
1259	-C=O bending	1353	N-H in plan deformation
1180,1128	-C-O- stretching	955	piranose ring
1083,1043	-OH bending	890	C-N finger print band
954	-CH3 rocking		
869,756,700	-C-C- stretching		

In Figure 6a, the UV-visible of PLA-based samples containing Ch and cCh are plotted. The UV-visible spectra do not show any significant difference between Ch- and cCh-containing systems, highlighting no change of the optical properties of PLA-based samples in comparison to that of pristine PLA matrix, in agreement with FTIR analysis. Only a negligible difference in the UV adsorption, *i.e.* 220-240 nm, is observed, but these small differences cannot be related to a variation of the structure, and subsequent to the properties. Additionally, to evaluate the film transparency, the linear attenuation coefficient (K), considering the absorbance values at 750 nm, has been calculated, and in Figure 6b, the K trend as a function of Ch concentration are plotted. The values of linear attenuation coefficients (K) have been calculated considering the measured absorption values (A) and

samples thickness (D), using the formula: $K = A/(2.3D)$ [43]. Although the differences are negligible, the transparency of the PLA-based films is slightly lower due to the presence of both Ch and cCh, and K values decrease with increasing the cCh concentration, see Figure 6b.
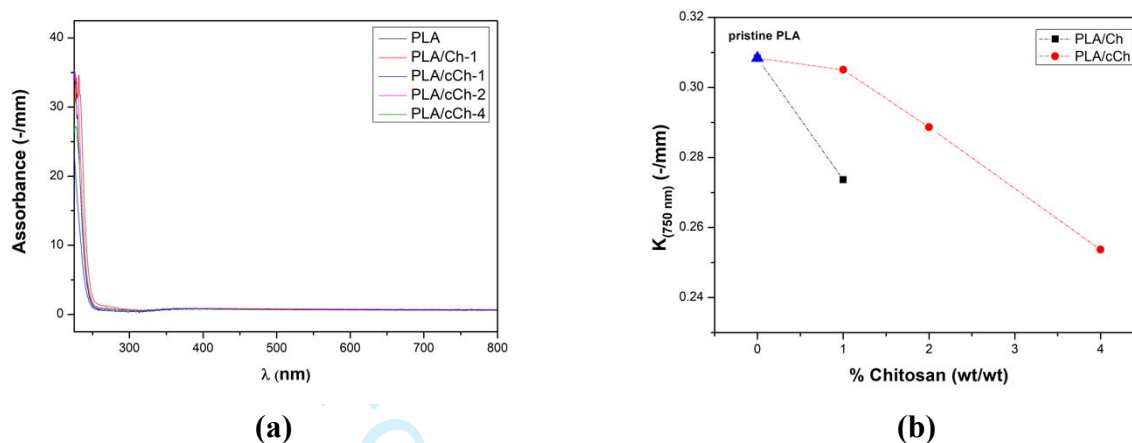

(a)

(b)

Figure 6. (a) UV-visible spectra of PLA-based samples containing Ch and cCh and (b) linear attenuation coefficient, K, as a function of Ch concentration

3.3. Accumulation of oxygen-containing groups in PLA/Ch and PLA/cCh

The PLA/Ch and PLA/cCh thin films (thickness 60 μm) are subjected to accelerated UVB exposure and the accumulation of oxygen-containing groups in time is monitored by FTIR analysis.

According to literature, the PLA oxidation degradation mechanism occurs predominantly by random chain scission of the polymer backbone, and in Figure 7a, main degradation mechanism is shown [19]. Besides, the oxidation of PLA-based nanocomposites in both melt state and solid state brings about a decrease of the PLA molar mass via pathway (1). The degradation pathways (2) and (3) would probably also occur, but the number of anhydrides species, possibly volatile, would be low and not detectable. Therefore, the increase of the PLA absorption band, due to the presence of anhydride functions at around 1845 cm^{-1} and related to the accumulation of oxygen-containing groups, can be profitable followed FTIR analysis.

As already pointed out, Ch degradation occurs mainly by depolymerization, *i.e.* chain fragmentation, due to deacetylation, and oxidation, see Figure 7b [34]. As widely documented in the literature, the new groups can react themselves, causing interchain crosslinking and *3D*-structure formation.
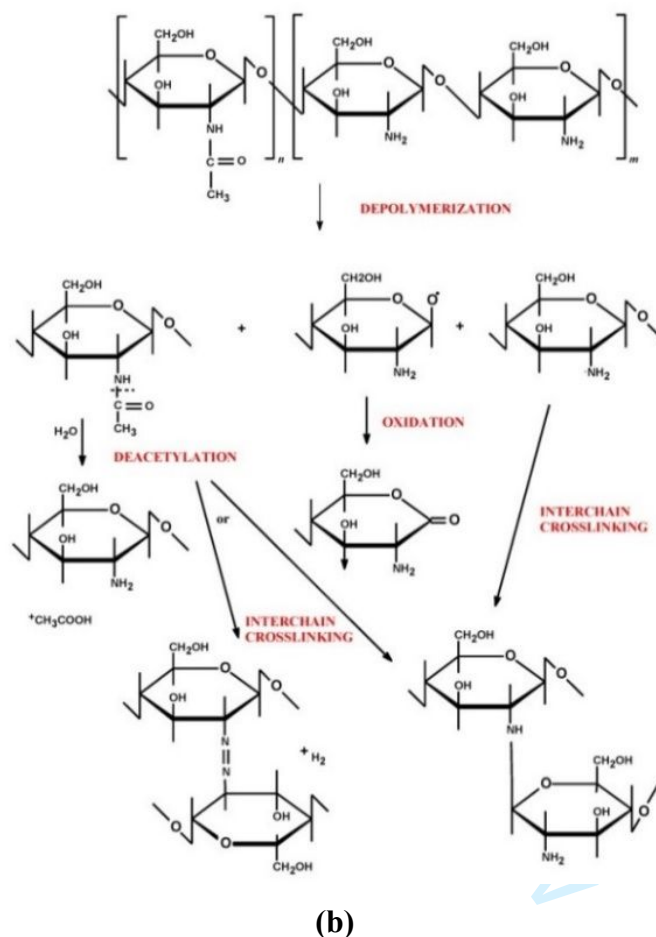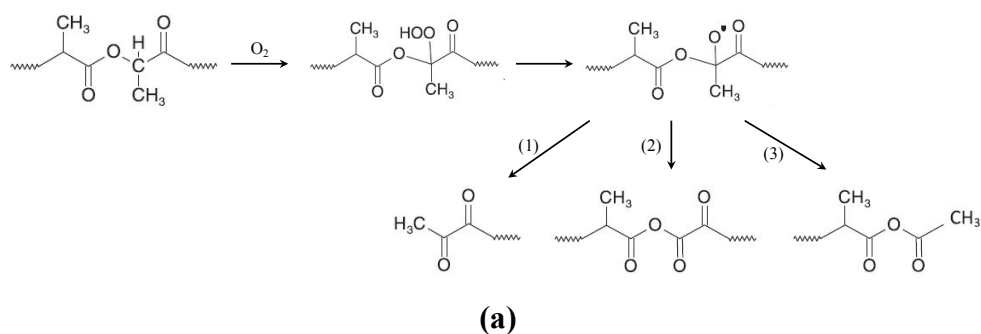
(a)

(b)

Figure 7. (a) PLA oxidation mechanism, involving β-scission of alkoxy radical according to [19] (b) Chitosan degradation mechanism through depolymerization [34]

As discussed above, the main FTIR absorption bands of PLA and Ch are overlapped, the detection of different peaks that can be attributed to degradation of PLA of Ch separately is very difficult, also considering that Ch and cCh addition is at low amount. To understand the photo-degradation process there is chosen to follow the variation of anhydride accumulations in PLA.

In Figure 8a-b, the variations of anhydride band area as a function of exposure time for all investigated PLA-based samples are shown, and all acquired FTIR spectra at different exposure times as supplementary file are reported. At short exposure times, up to 400h, the anhydride accumulation

is more pronounced for neat PLA, rather than for PLA/Ch-1, see Figure 8a. Interestingly, at longer exposure times, up to 1000h, the anhydride accumulation becomes more pronounced for PLA/Ch-1, in comparison to the neat PLA. As for the un-treated chitosan, the addition of crosslinked chitosan at short exposure time slow down the anhydride accumulation PLA, while at long exposure time results in accelerations of anhydride accumulation. Specifically, the cross over between PLA and PLA/cCh-1.0, 2.0, 4.0 %w occurs respectively at 80, 170 and 260 h. Thus, the addition of crosslinked chitosan results in better pro-degradation action then than blended chitosan. Moreover, it is worth noting that the trends of accumulation of anhydride functions increase with increasing the cCh concentration and this trend is particularly pronounced at long exposure times for the higher concentration, see Figure 8b. Probably at short exposure time the radicals coming from chitosan depolymerization interact with the free radicals coming from β-scission of PLA. Over a certain time, that depends of chitosan concentration and of chitosan chemical structure (un-treated and crosslinked chitosan), the presence of chitosan radicals accelerates the β-scission of PLA.
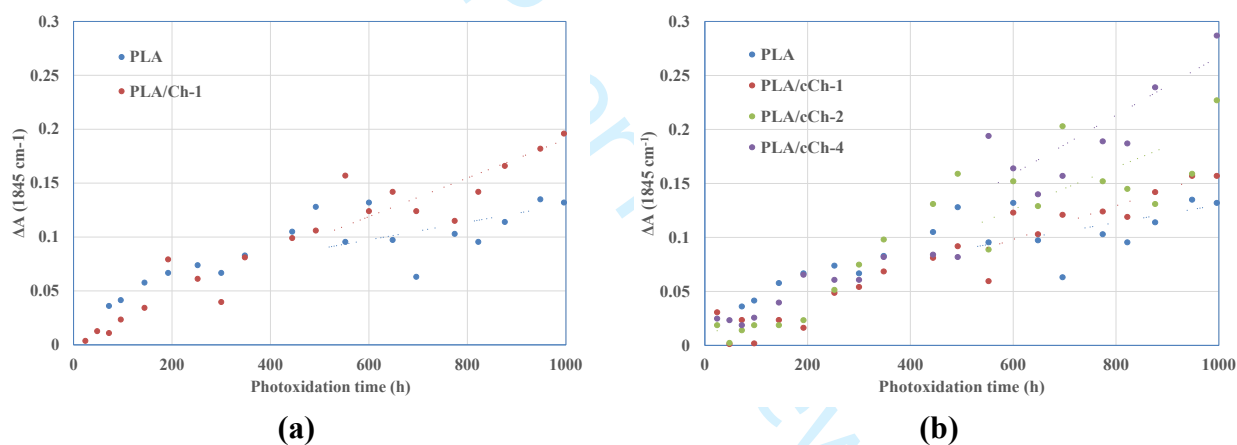

Figure 8. Analysis of anhydride accumulation as a function of UVB exposure time for PLA-based samples containing Ch

4. Conclusions

An innovative sustainable approach to induce and control end-of-life oxygen-containing group accumulation in biopolyester, such as polylactic acid, through introduction of polysaccharide particles, such as chitosan, is proposed. The chitosan has been subjected to ionotropically crosslinking to obtain micro-/nano-particles, and these particles, at different concentration, have been introduced in PLA matrix through melt mixing. The crosslinked chitosan particles do not significantly modify the thermal behaviour, spectroscopic properties and morphology of PLA, while untreated chitosan, although at low concentration, has a pronounced effect on the PLA properties and performance.

To evaluate the oxygen-containing group accumulation, thin PLA films without and with Ch and cCh, have been subjected to accelerated UVB exposure and the accumulation of anhydride functions,

coming from the PLA photo-degradation, has been monitored through FTIR analysis in time. Obtained results suggests that, although at short exposure time, the anhydride accumulation is more pronounced for neat PLA, rather than for both PLA/Ch and PLA/cCh, the pro-degradant effect of both Ch and cCh is well noticeable at long exposure time. Therefore, it is worth noting that the trends of accumulation of anhydride functions increase with increasing of the cCh concentration suggesting a successful induction and control of the oxygen-containing groups accumulation at biopolyester end-of-life.

References

1. Jamshidian, M., Tehrany, E.A., Imran, M., Jacquot, M., and Desobry, S. (2010) Poly-Lactic Acid: Production, applications, nanocomposites, and release studies. *Compr. Rev. Food Sci. Food Saf.*, **9** (5), 552–571.

2. Lim, L.T., Auras, R., and Rubino, M. (2008) Processing technologies for poly(lactic acid). *Prog. Polym. Sci.*, **33** (8), 820–852.

3. Di Bartolo, A., Infurna, G., and Dintcheva, N.T. (2021) A Review of Bioplastics and Their Adoption in the Circular Economy. *Polymers (Basel).*, **13** (8), 1229.

4. Vroman, I., and Tighzert, L. (2009) Biodegradable polymers. *Materials (Basel).*, **2** (2), 307–344.

5. Theinsathid, P., Chandrachai, A., and Keeratipibul, S. (2009) Managing bioplastics business innovation in start up phase. *J. Technol. Manag. Innov.*, **4** (1), 82–93.

6. Yew, G.H., Mohd Yusof, A.M., Mohd Ishak, Z.A., and Ishiaku, U.S. (2005) Water absorption and enzymatic degradation of poly(lactic acid)/rice starch composites. *Polym. Degrad. Stab.*, **90** (3), 488–500.

7. Tokiwa, Y., and Calabia, B.P. (2007) Biodegradability and biodegradation of polyesters. *J. Polym. Environ.*, **15** (4), 259–267.

8. Cai, X., Tong, H., Shen, X., Chen, W., Yan, J., and Hu, J. (2009) Preparation and characterization of homogeneous chitosan-polylactic acid/hydroxyapatite nanocomposite for bone tissue engineering and evaluation of its mechanical properties. *Acta Biomater.*, **5** (7), 2693–2703.

9. Panos, I., Acosta, N., and Heras, A. (2008) New Drug Delivery Systems Based on Chitosan. *Curr. Drug Discov. Technol.*, **5** (4), 333–341.

10. McLauchlin, A.R., and Thomas, N.L. (2009) Preparation and thermal characterisation of poly(lactic acid) nanocomposites prepared from organoclays based on an amphoteric surfactant. *Polym. Degrad. Stab.*, **94** (5), 868–872.

11. Wu, T.M., and Wu, C.Y. (2006) Biodegradable poly(lactic acid)/chitosan-modified montmorillonite nanocomposites: Preparation and characterization. *Polym. Degrad. Stab.*, **91** (9), 2198–2204.

12. Azeredo, H.M.C. d. (2009) Nanocomposites for food packaging applications. *Food Res. Int.*, **42** (9), 1240–1253.

13. Nanda, R., Sasmal, A., and Nayak, P.L. (2011) Preparation and characterization of chitosan-polylactide composites blended with Cloisite 30B for control release of the anticancer drug paclitaxel. *Carbohydr. Polym.*, **83** (2), 988–994.

14. Chouwatat, P., Polsana, P., Noknoi, P., Siralertmukul, K., and Srikulkit, K. (2010) Preparation of Hydrophobic Chitosan Using Complexation Method for PLA/Chitosan Blend. *J. Met. Mater. Miner.*, **20** (1), 41–44.

15. Cheng, Y., Deng, S., Chen, P., and Ruan, R. (2009) Polylactic acid (PLA) synthesis and modifications: A review. *Front. Chem. China*, **4** (3), 259–264.

16. Sionkowska, A., Planecka, A., Kozlowska, J., Skopinska-Wisniewska, J., and Los, P. (2011) Weathering of chitosan films in the presence of low- and high-molecular weight additives. *Carbohydr. Polym.*, **84** (3), 900–906.

17. Zaidi, L., Kaci, M., Bruzaud, S., Bourmaud, A., and Grohens, Y. (2010) Effect of natural weather on the structure and properties of polylactide/Cloisite 30B nanocomposites. *Polym. Degrad. Stab.*, **95** (9), 1751–1758.

18. Dintcheva, N.T., Arrigo, R., Baiamonte, M., Rizzarelli, P., and Curcuruto, G. (2017) Concentration-dependent anti-/pro-oxidant activity of natural phenolic compounds in bio-polyesters. *Polym. Degrad. Stab.*, **142**, 21–28.

19. Dintcheva, N.T., Baiamonte, M., and Spera, M. (2018) Assessment of pro-oxidant activity of natural phenolic compounds in bio-polyesters. *Polym. Degrad. Stab.*, **152**, 280–288.

20. Dintcheva, N.T., and D'anna, F. (2019) Anti-/pro-oxidant behavior of naturally occurring molecules in polymers and biopolymers: A brief review. *ACS Sustain. Chem. Eng.*, **7** (15), 12656–12670.

21. Tsuji, H., Echizen, Y., and Nishimura, Y. (2006) Photodegradation of biodegradable polyesters: A comprehensive study on poly(l-lactide) and poly(ε-caprolactone). *Polym. Degrad. Stab.*, **91** (5), 1128–1137.

22. La Mantia, F.P., Dintcheva, N.T., Malatesta, V., and Pagani, F. (2006) Improvement of photo-stability of LLDPE-based nanocomposites. *Polym. Degrad. Stab.*, **91** (12), 3208–3213.

23. Dintcheva, N.T., Al-Malaika, S., and La Mantia, F.P. (2009) Effect of extrusion and photo-oxidation on polyethylene/clay nanocomposites. *Polym. Degrad. Stab.*, **94** (9), 1571–1588.

24. Dintcheva, N.T., Gennaro, D., Teresi, R., and Baiamonte, M. (2019) Pro-degradant activity of naturally occurring compounds on polyethylene in accelerate weathering conditions. *Materials (Basel).*, **12** (1).

25. Elsabee, M.Z., and Abdou, E.S. (2013) Chitosan based edible films and coatings: A review. *Mater. Sci. Eng. C*, **33** (4), 1819–1841.

26. Guo, Z., Xing, R., Liu, S., Zhong, Z., Ji, X., Wang, L., and Li, P. (2008) The influence of molecular weight of quaternized chitosan on antifungal activity. *Carbohydr. Polym.*, **71** (4), 694–697.

27. Souza, H.K.S., Campiña, J.M., Sousa, A.M.M., Silva, F., and Gonçalves, M.P. (2013) Ultrasound-assisted preparation of size-controlled chitosan nanoparticles: Characterization and fabrication of transparent biofilms. *Food Hydrocoll.*, **31** (2), 227–236.

28. Branca, C., D'Angelo, G., Crupi, C., Khouzami, K., Rifici, S., Ruello, G., and Wanderlingh, U. (2016) Role of the OH and NH vibrational groups in polysaccharide-nanocomposite interactions: A FTIR-ATR study on chitosan and chitosan/clay films. *Polymer (Guildf).*, **99**, 614–622.

29. Epure, V., Griffon, M., Pollet, E., and Avérous, L. (2011) Structure and properties of glycerol-plasticized chitosan obtained by mechanical kneading. *Carbohydr. Polym.*, **83** (2), 947–952.

30. Sun, S., Wang, Y., Li, L., Huang, Z., and Zhou, H. (2020) Thermoplastic biomass transparent films directly fabricated by chitosan nanospheres. *Polymer (Guildf).*, **192** (February), 122335.

31. Aranaz, I., Mengibar, M., Harris, R., Panos, I., Miralles, B., Acosta, N., Galed, G., and Heras, A. (2012) Functional Characterization of Chitin and Chitosan. *Curr. Chem. Biol.*, **3** (2), 203–230.

32. Bastioli, C. (2005) *Handbook of Biodegradable Polymers*, Shropshire, UK.

33. Ebnesajjad, S. (2012) *Handbook of Biopolymers and Biodegradable Plastics, Properties, Processing and Applications*, Amsterdam, The Netherlands.

34. Szymańska, E., and Winnicka, K. (2015) Stability of chitosan - A challenge for pharmaceutical and biomedical applications. *Mar. Drugs*, **13** (4), 1819–1846.

35. Adrian, G., Mihai, M., and Vodnar, D.C. (2019) The Use of Chitosan , Alginate , and Pectin in the. *Polymers (Basel).*, **11**, 1837.

36. Infurna, G., Cavallaro, G., Lazzara, G., Milioto, S., and Dintcheva, N.T. (2021) Understanding the effects of crosslinking and reinforcement agents on the performance and durability of biopolymer films for cultural heritage protection. **42**, 1–11.

37.   Sun, L., Sun, J., Chen, L., Niu, P., Yang, X., and Guo, Y. (2017) Preparation and characterization of chitosan film incorporated with thinned young apple polyphenols as an active packaging material. *Carbohydr. Polym.*, **163** (17), 81–91.

38.   Zawadzki, J., and Kaczmarek, H. (2010) Thermal treatment of chitosan in various conditions. *Carbohydr. Polym.*, **80** (2), 394–400.

39.   Auras, R., Harte, B., and Selke, S. (2004) An overview of polylactides as packaging materials. *Macromol. Biosci.*, **4** (9), 835–864.

40.   Gupta, B., Revagade, N., and Hilborn, J. (2007) Poly(lactic acid) fiber: An overview. *Prog. Polym. Sci.*, **32** (4), 455–482.

41.   Sodergard, A., and Stolt, M. (2002) Properties of polylactic acid fiber based polymers and their correlation with composition. *Prog. Polym. Sci.*, **27**, 1123–1163.

42.   Matet, M., Heuzey, M.C., Pollet, E., Ajji, A., and Avérous, L. (2013) Innovative thermoplastic chitosan obtained by thermo-mechanical mixing with polyol plasticizers. *Carbohydr. Polym.*, **95** (1), 241–251.

43.   Infurna, G., Cavallaro, G., Lazzara, G., Milioto, S., and Dintcheva, N.T. (2021) Understanding the Effects of Crosslinking and Reinforcement Agents on the Performance and Durability of Biopolymer Films for Cultural Heritage Protection. *Molecules*, **26**, 3468.